

OPEN ACCESS

The role of space charge in spin-resolved photoemission experiments

To cite this article: A Fognini *et al* 2014 *New J. Phys.* **16** 043031

View the [article online](#) for updates and enhancements.

You may also like

- [Operating synchrotron light sources with a high gain free electron laser](#)
S Di Mitri and M Cornacchia
- [AMO science at the FLASH and European XFEL free-electron laser facilities](#)
J Feldhaus, M Krikunova, M Meyer et al.
- [X-ray free-electron lasers: from dreams to reality](#)
C Pellegrini

The role of space charge in spin-resolved photoemission experiments

A Fognini¹, G Salvatella¹, T U Michlmayr¹, C Wetli¹, U Ramsperger¹,
T Bähler¹, F Sorgenfrei², M Beye², A Eschenlohr^{2,8}, N Pontius², C Stamm^{2,3},
F Hieke⁴, M Dell'Angela⁴, S de Jong⁵, R Kukreja⁵, N Gerasimova^{6,9},
V Rybnikov⁶, H Redlin⁶, J Raabe⁷, A Föhlisch², H A Dürr⁵, W Wurth⁴,
D Pescia¹, A Vaterlaus¹ and Y Acremann¹

¹Laboratory for Solid State Physics, ETH Zurich, 8093 Zurich, Switzerland

²Institut für Methoden und Instrumentierung der Forschung mit Synchrotronstrahlung, Helmholtz-Zentrum Berlin für Materialien und Energie GmbH, D-12489 Berlin, Germany

³Department of Materials, ETH Zurich, 8093 Zurich, Switzerland

⁴Institut für Experimentalphysik and Center for Free-Electron Laser Science, Universität Hamburg, D-22607 Hamburg, Germany

⁵SLAC National Accelerator Laboratory, Menlo Park, CA 94025, USA

⁶DESY, D-22607 Hamburg, Germany

⁷Paul Scherrer Institute, 5232 Villigen, Switzerland

⁸Universität Duisburg-Essen, Fakultät für Physik, D-47048 Duisburg, Germany

⁹European XFEL GmbH, D-22761 Hamburg, Germany

E-mail: afognini@phys.ethz.ch

Received 21 October 2013, revised 14 February 2014

Accepted for publication 3 March 2014

Published 30 April 2014

New Journal of Physics **16** (2014) 043031

[doi:10.1088/1367-2630/16/4/043031](https://doi.org/10.1088/1367-2630/16/4/043031)

Abstract

Spin-resolved photoemission is one of the most direct ways of measuring the magnetization of a ferromagnet. If all valence band electrons contribute, the measured average spin polarization is proportional to the magnetization. This is even the case if electronic excitations are present, and thus is of particular interest for studying the response of the magnetization to a pump laser pulse. Here, we demonstrate the feasibility of ultrafast spin-resolved photoemission using free electron laser (FEL) radiation and investigate the effect of space charge on the detected spin polarization. The sample is exposed to the radiation of the FEL FLASH in Hamburg. Surprisingly, the measured spin polarization depends on the fluence of the FEL radiation: a higher FEL fluence reduces the



Content from this work may be used under the terms of the [Creative Commons Attribution 3.0 licence](https://creativecommons.org/licenses/by/3.0/). Any further distribution of this work must maintain attribution to the author(s) and the title of the work, journal citation and DOI.

measured spin polarization. Space-charge simulations can explain this effect. These findings have consequences for future spin-polarized photoemission experiments using pulsed photon sources.

Keywords: spin-polarized photoemission, free electron laser radiation, space charge

1. Introduction

Photoemission spectroscopy allows for direct access to the band structure of a solid [1, 2]. Modern vacuum ultraviolet (VUV) and x-ray sources enable high-resolution angular resolved photoelectron spectroscopy [3, 4], allowing for imaging of the Fermi surface. Photoelectron spectroscopy can be extended by a spin detector in order to resolve the spin-split band structure of magnetic samples [5–7]. This way, the electronic origin of magnetism can be directly observed. The next frontier is to extend photoelectron spectroscopy into the time domain to study the dynamics of the electron and spin systems [8]. In a corresponding pump-probe experiment, the photon energy of the pulsed light source is essential as it determines which part of the band structure can be accessed. Titanium sapphire lasers combined with third and fourth harmonic generation stages as well as two-photon photoemission experiments offer the possibility to investigate electron dynamics close to the Fermi energy [9–11]. The development of higher harmonic generation sources [12–15] extends laser-based femtosecond light sources to the VUV range. Still, due to the limited photon flux of laser-based sources, ultrafast spin-resolved photoemission from the entire valence band is difficult to achieve. Here, we present an experiment investigating the feasibility of photoemission with spin analysis using free electron laser (FEL) radiation. FEL radiation provides the short pulses, the high photon flux, as well as the photon energy required for spin- and time-resolved photoemission experiments. However, FELs are challenging sources, especially in the case of photoemission experiments [16]: in classical photoemission experiments the usual flux of the source is rarely higher than 10^{14} photons per second (e.g. a synchrotron source). At these conditions, the number of generated photoelectrons at any time is low enough that they hardly interact with each other. In contrast, the peak intensity during the femtosecond FEL pulses is several orders of magnitude larger. This large number of quasi-simultaneously emitted photoelectrons causes a space-charge cloud in front of the sample, which then causes a distortion and shifting of the detected photoelectron spectra [16]. In contrast, for energy-integrated yet spin-resolved experiments, one would not expect space-charge effects to affect the detected spin polarization: once the electrons are in vacuum, electron–electron scattering will not affect the total spin angular momentum of the electron cloud. Therefore, the average spin polarization of the photoelectrons is expected to remain independent of space-charge effects. This conjecture is experimentally tested at the PG2 beamline [17, 18] of the free electron laser in Hamburg (FLASH).

2. Experimental setup

The principle of the experiment is shown in figure 1. An iron film on tungsten (110) serves as the magnetic sample.

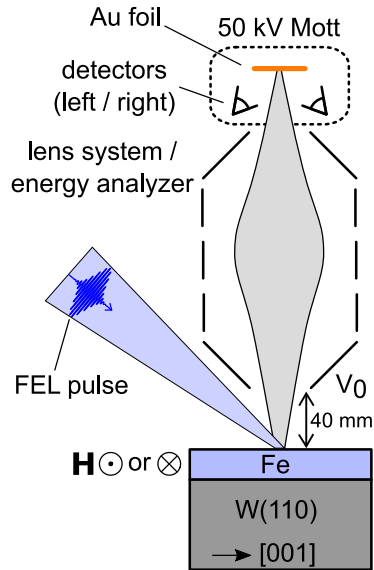


Figure 1. Experimental overview: the iron film is probed by FEL pulses, which generate an electron cascade. An electric field of 22 kV m^{-1} applied between the sample and the first lens element accelerates the electrons towards the first lens element. The spin polarization is measured with a Mott detector.

2.1. Sample preparation

The tungsten single crystal is cleaned by oxygen annealing and subsequent high-temperature treatment in an ultra-high vacuum. After cooling down to room temperature, a 15 monolayer film of iron is deposited by evaporation at a pressure of 10^{-10} mbar. Details of the sample preparation process have been published previously [19]. The single crystalline iron film has a magnetic in-plane easy axis along the $[\underline{1}10]$ direction and yields, after being brought to magnetic saturation, a magnetic single domain remanent state [19].

2.2. Excitation of the sample

After preparation, the sample is transferred *in situ* into the measurement chamber. A pulsed magnet is used to switch the magnetization of the sample. Its pulses have a maximum field strength of 300 Oe and a pulse length of $15 \mu\text{s}$. During the measurement, the sample environment is field free and the sample magnetization $M_{\uparrow,\downarrow}$ remains in remanence. The sample can be probed by FEL pulses of ≈ 50 fs full width half maximum average length at a photon energy of 182 eV. The pulse length was determined from the photon spectra and the dispersion properties of the PG2 beamline. The FEL pulse energy on the sample fluctuates in the range of 6–300 nJ per pulse, and the FEL impinges under 45° onto the sample. The spot size of the FEL beam on the sample is $130 \times 150 \mu\text{m}^2$. In addition, the measurement chamber is equipped with an electron gun to perform static measurements.

2.3. Electron optics and spin detection

The FEL pulses or the electron gun create electron emission from the sample. The electrons that actually leave the sample mostly originate from the iron film as the inelastic mean free path is

shorter than the film thickness [20]. The cascade electrons are collected by an electrostatic lens system, which provides no energy analysis. This lens system can be replaced by a hemispherical energy analyzer for the energy resolved experiments. A Mott spin polarimeter is used in both cases to detect the spin polarization along the magnetization direction of the sample. Inside the Mott polarimeter, the electrons are accelerated to 50 keV and scattered on a gold foil 80 nm thick. The scattered electrons are detected by passivated implanted planar silicon (PIPS) detectors. They provide a voltage pulse proportional to the deposited energy. In the case of experiments using the continuous beam from the electron gun, we detect less than one electron within the dead time of the PIPS detectors. Therefore, conventional electron counting is used. A discriminator circuit is used to select events from elastically scattered electrons only. The polarization can be determined as [5]

$$P = \frac{1}{S_e} \frac{\sqrt{N_{\text{left}}^{\uparrow} N_{\text{right}}^{\downarrow}} - \sqrt{N_{\text{left}}^{\downarrow} N_{\text{right}}^{\uparrow}}}{\sqrt{N_{\text{left}}^{\uparrow} N_{\text{right}}^{\downarrow}} + \sqrt{N_{\text{left}}^{\downarrow} N_{\text{right}}^{\uparrow}}}, \quad (1)$$

where $N_{\text{left,right}}^{\uparrow,\downarrow}$ is the electron count rate for the right- and left-detector channel and magnetization directions $M_{\uparrow,\downarrow}$. $S_e = 0.17$ is the Sherman factor, which characterizes the sensitivity of our spin polarimeter.

In the case of experiments using FEL radiation, the situation is different as electrons are emitted by short VUV pulses. More than one electron per pulse can reach the PIPS detectors, and single electron counting becomes impossible. Therefore, it is not possible to discriminate between elastically and inelastically scattered electrons. However, the PIPS detectors provide an electrical pulse height $I_{\text{left,right}}^{\uparrow,\downarrow}$ proportional to the *total* number of electrons per FEL pulse.

From the averaged pulse heights, the electron polarization P is calculated by replacing the count rates in equation (1) by the corresponding pulse heights:

$$P = \frac{1}{S_{\text{FEL}}} \frac{\sqrt{I_{\text{left}}^{\uparrow} I_{\text{right}}^{\downarrow}} - \sqrt{I_{\text{left}}^{\downarrow} I_{\text{right}}^{\uparrow}}}{\sqrt{I_{\text{left}}^{\uparrow} I_{\text{right}}^{\downarrow}} + \sqrt{I_{\text{left}}^{\downarrow} I_{\text{right}}^{\uparrow}}}. \quad (2)$$

Here, the Sherman factor S_{FEL} is calibrated with measurements at a FEL pulse energy of $E_{\text{pulse}} < 1.5 \mu\text{J cm}^{-2}$. The result is scaled to match that obtained with the electron gun. This way, S_{FEL} is determined to be 0.1. The reduction in the Sherman factor S_{FEL} compared to S_e is due to the inelastically scattered electrons included in the FEL-based measurement.

3. The influence of FEL pulse energy on measured spin polarization

In principle, one would not expect the measured magnetization to be affected by the FEL pulse itself: the maximum pulse energy per unit area of the FEL beam in this experiment is two orders of magnitude smaller than needed by near infrared pump lasers to demagnetize the sample [8]. Nevertheless, one finds a threshold FEL pulse energy density of about $10 \mu\text{J cm}^{-2}$, above which P is gradually reduced; see figure 2(a). Since the sample does not get demagnetized by the FEL pulse, the detection method itself must be influenced by the pulse energy. Note that the FEL-based experiments were performed without electron energy analysis.

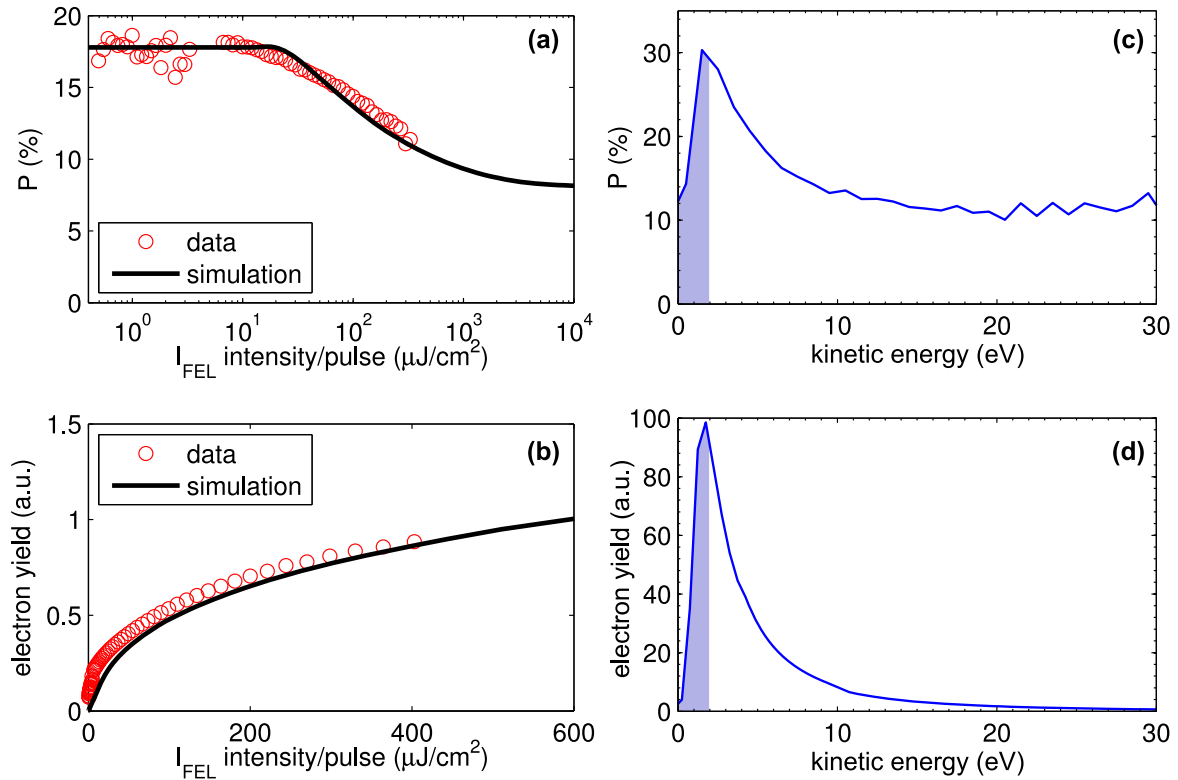


Figure 2. (a) FEL intensity-resolved polarization measurement. The dots show the measurement of the spin polarization for a 15 monolayer thick iron film, and the black line corresponds to the space-charge simulation result. (b) The number of detected electrons as a function of the FEL pulse energy. The black line shows the space-charge simulation result. (c), (d) The polarization and yield of the secondary electron cascade, excited with an electron gun at 4 kV primary energy, showing the enhanced spin polarization for low-energy cascade electrons. The shaded area highlights the part of the spectrum that is suppressed by space charge. The higher the space charge, the more low-energetic electrons are hindered from escaping the sample.

3.1. The role of space charge

The high peak intensity of the FEL is challenging for all photoemission experiments [16]: the immediate release of electrons from the sample causes a cloud of electrons in front of the sample. The Coulomb interaction within the space-charge cloud alters the photoemission spectrum. The space charge can even reduce the photoelectron yield as seen in figure 2(b): without space-charge effects, one would expect a linear dependence between the number of detected electrons and the FEL pulse energy, in contrast to the observed behavior. The question then arises as to whether the space charge can also affect the detected spin polarization. To address this question, we need to know which electrons are repelled by the space-charge cloud. Intuitively, one expects that lower energy electrons are predominantly suppressed by the Coulomb force of the cloud as they need the least momentum transfer to change their trajectories. If the spin polarization of the cascade electrons depends on their kinetic energy, the space charge can indeed affect the polarization of the detected electrons.

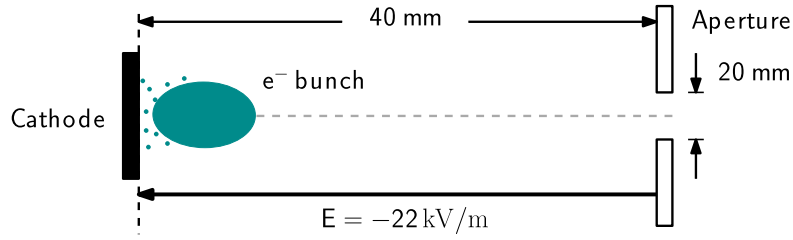


Figure 3. Geometry of the simulation: the electrons are emitted from a photo cathode and are accelerated towards an aperture. The aperture corresponds to the size of the first element of the electrostatic lens system.

Figures 2(c) and (d) show the energy dependence of the spin polarization and emission current from our sample, excited with a continuous electron beam of 4 keV primary energy, providing a space-charge free reference. These measurements have been performed in the same experimental chamber. In order to detect spin-polarized spectra, a hemispherical energy analyzer is used in front of the Mott detector. The polarization peak at ≈ 2 eV is caused by the well-known spin filter effect [21]. If the space charge reduces the amount of these low energy but highly polarized electrons, the polarization reduction observed in the FEL experiments could be explained solely by a space-charge effect.

3.2. Space-charge simulation

To quantify the above ideas, we simulate the space-charge effect using the tracking algorithm *astra*¹⁰, which solves the electric field of the electron cloud and computes the particle trajectories. The initial spatial distribution of particles at the cathode is chosen to follow a Gaussian profile of $\sigma_x = \sigma_y = 50 \mu\text{m}$, the approximate spot size of the FEL beam; see figure 3. The cathode randomly deploys charged particles. The temporal profile of the sample current is assumed to be an exponentially decaying function with a time constant of $\tau = 100$ fs. This time accounts for the FEL pulse length and the formation time of the cascade [22]. The initial photoelectron spectrum $N_{\text{in}}(E_{\text{kin}})$ and its corresponding polarization $P_{\text{in}}(E_{\text{kin}})$ are taken from the measurements shown in figures 2(c), (d). The particles leaving the cathode are accelerated by a static electric field of $E = 22 \text{ kV m}^{-1}$, provided by the potential difference between the sample and the first lens element of the electron optic system. The simulation deploys electrons randomly drawn from the initial spectrum and calculates their trajectories influenced by the space charge. An aperture corresponding to the entrance of our electrostatic lens is included. The simulation is undertaken as a function of the total emitted charge, $Q = 10^{-6} - 10^{-1}$ nC, corresponding to $N = 10^4 - 10^9$ emitted electrons per pulse. The result is the spin-polarized photoelectron spectrum at the entrance of the electrostatic lens system, which is modeled by the aperture.

3.3. ASTRA simulation results

Figure 4 shows the simulated spectra at the entrance of the lens system as a function of the *initial* kinetic energy. The spectra are shown for different total emitted charge values. For low

¹⁰ Available at <http://www.desy.de/~mpyflo/>

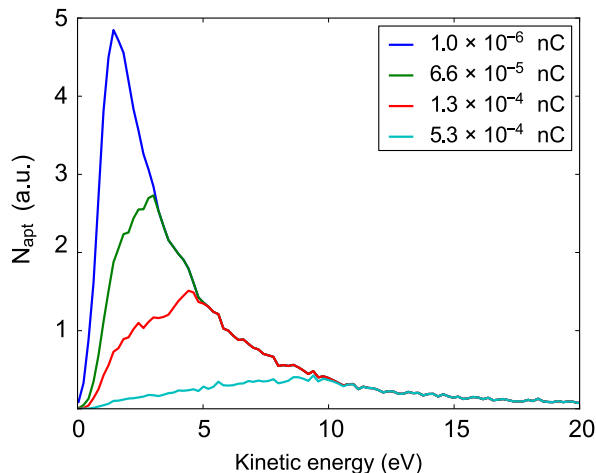


Figure 4. The spectrum of simulated electrons that pass through the space charge cloud and enter the electron lens, for different total charge values. The spectra have been scaled by the total charge values. For that reason, all spectra match up above 10 eV.

values of the emitted charge, the space-charge effect is negligible and the final spectrum is essentially the same as the initial one. As the total charge increases, the space-charge effect develops. Lower energy electrons are held back by the space-charge cloud and can not reach the lens entrance. The acquired spectra are now used to calculate the spin polarization of the remaining electrons.

3.4. Calculated reduction of the detected polarization

Based on the simulation, we know the probability

$$w(E, I) = \frac{N_{\text{apt}}(E, I)}{N_{\text{in}}(E, I)} \quad (3)$$

that an electron reaches the aperture. Notice that E denotes the *initial* kinetic energy of the electrons. I is the pulse energy of the FEL, and N_{apt} is the number of electrons reaching the aperture. With the measured initial polarization distribution $P_{\text{in}}(E)$, we obtain the resulting spin polarization at the aperture as

$$P_{\text{sim}}(I) = \frac{1}{\Delta E} \int_0^{\Delta E} P_{\text{in}}(E) w(E, I) dE \quad (4)$$

with $\Delta E = 30$ eV. The bound is given by the width of the measured initial energy spectrum and covers the most significant part of the cascade electrons.

The simulated polarization $P_{\text{sim}}(I)$ decreases from 18% to 10% within an emitted charge range of 10^3 nC, visible in the simulation curve in figure 2(a). The only fitting parameter in our simulation is the total number of emitted electrons per absorbed photon of 0.07. Comparison of the simulations with the measured polarization from the FEL source shows that the space-charge effect can account for the loss of polarization in the FEL-based photoemission experiment.

4. Conclusion

Our experiment shows that the measured spin polarization can be affected by space-charge effects, therefore limiting the number of usable photons per pulse at ultrafast x-ray and VUV sources. Space-charge effects can be reduced by increasing the FEL spot size, which in turn requires a higher pump pulse energy to excite the sample in a pump-probe configuration. An improvement in detector efficiency would allow us to decrease the probe flux and still provide enough photoelectrons for measurement. Novel spin detectors utilizing an elastic scattering of electrons on analyzer crystals combined with parallel detection can be used to enhance the detection efficiency by several orders of magnitude [23]. In addition, it is essential to utilize sources with a higher pulse repetition rate and reduced number of photons per pulse. FLASH is exceptionally suited to spin-resolved photoemission experiments as the superconducting linear accelerator structure allows for longer pulse trains than conventional linear accelerators. Future high-repetition-rate superconducting FELs [24] and laser driven higher harmonic sources will allow for direct insight into the femtosecond dynamics of the spin and electron systems of solids.

Acknowledgments

This work was supported by the Swiss National Science Foundation, ETH Zurich and the Volkswagen-Stiftung. We also acknowledge support from the DFG through SFB 925 and the BMBF priority program FSP 301 'FLASH'. Research at Stanford was supported through the Stanford Institute for Materials and Energy Science (SIMES) under contract DE-AC02-76SF00515. Significant portions of this research were carried out at the light source FLASH at DESY, a member of the Helmholtz Association (HGF). We specially thank the machine operators and run coordinators at FLASH.

References

- [1] Hagström S, Nordling C and Siegbahn K 1964 Electron spectroscopy for chemical analyses *Phys. Lett.* **9** 235–6
- [2] Hüfner S 2003 *Photoelectron Spectroscopy: Principles and Applications* 3rd edn (Berlin: Springer)
- [3] Zhou X J, Bogdanov P, Kellar S A, Noda T, Eisaki H, Uchida S, Hussain Z and Shen Z-X 1999 One-dimensional electronic structure and suppression of d-wave node state in $(\text{La}_{1.28}\text{Nd}_{0.6}\text{Sr}_{0.12})\text{CuO}_4$ *Science* **286** 268–72
- [4] Damascelli A, Hussain Z and Shen Z-X 2003 Angle-resolved photoemission studies of the cuprate superconductors *Rev. Mod. Phys.* **75** 473–541
- [5] Johnson P D 1997 Spin-polarized photoemission *Rep. Prog. Phys.* **60** 1217
- [6] Jozwiak C, Graf J, Lebedev G, Andresen N, Schmid A K, Fedorov A V, El Gabaly F, Wan W, Lanzara A and Hussain H 2010 A high-efficiency spin-resolved photoemission spectrometer combining time-of-flight spectroscopy with exchange-scattering polarimetry *Rev. Sci. Instrum.* **81** 053904
- [7] Hoesch M, Greber T, Petrov V N, Muntwiler M, Hengsberger M, Auwärter W and Osterwalder J 2002 Spin-polarized fermi surface mapping *J. Electron Spectrosc. Relat. Phenom.* **124** 263–79
- [8] Beaupaire E, Merle J-C, Daunois A and Bigot J-Y 1996 Ultrafast spin dynamics in ferromagnetic nickel *Phys. Rev. Lett.* **76** 4250–3

- [9] Vaterlaus A, Beutler T and Meier F 1991 Spin-lattice relaxation time of ferromagnetic gadolinium determined with time-resolved spin-polarized photoemission *Phys. Rev. Lett.* **67** 3314–7
- [10] Scholl A, Baumgarten L, Jacquemin R and Eberhardt W 1997 Ultrafast spin dynamics of ferromagnetic thin films observed by fs spin-resolved two-photon photoemission *Phys. Rev. Lett.* **79** 5146–9
- [11] Carley R, Döbrich K, Frietsch B, Gahl C, Teichmann M, Schwarzkopf O, Wernet P and Weinelt M 2012 Femtosecond laser excitation drives ferromagnetic gadolinium out of magnetic equilibrium *Phys. Rev. Lett.* **109** 057401
- [12] Zhou J, Peatross J, Murnane M M, Kapteyn H C and Christov I P 1996 Enhanced high-harmonic generation using 25 fs laser pulses *Phys. Rev. Lett.* **76** 752–5
- [13] Zaïr A *et al* 2008 Quantum path interferences in high-order harmonic generation *Phys. Rev. Lett.* **100** 143902
- [14] Shiner A D, Trallero-Herrero C, Kajumba N, Bandulet H-C, Comtois D, Légaré F, Giguère M, Kieffer J-C, Corkum P B and Villeneuve D M 2009 Wavelength scaling of high harmonic generation efficiency *Phys. Rev. Lett.* **103** 073902
- [15] Bucksbaum P H 2007 The future of attosecond spectroscopy *Science* **317** 766–9
- [16] Pietzsch A *et al* 2008 Towards time resolved core level photoelectron spectroscopy with femtosecond x-ray free-electron lasers *New J. Phys.* **10** 033004
- [17] Martins M, Wellhofer M, Hoefl J T, Wurth W, Feldhaus J and Follath R 2006 Monochromator beamline for flash *Rev. Sci. Instrum.* **77** 115108–6
- [18] Gerasimova N, Dziarzhyski S and Feldhaus J 2011 *J. Mod. Opt.* **58** 1480
- [19] Miesch S, Fognini A, Acremann Y, Vaterlaus A and Michlmayr T U 2011 Fe on W(110), a stable magnetic reference system *J. Appl. Phys.* **109** 013905
- [20] Zdyb R and Bauer E 2013 Spin-resolved inelastic mean free path of slow electrons in Fe *J. Phys.: Condens. Matter* **25** 272201
- [21] Stöhr J and Siegmann H C 2006 *Magnetism, From Fundamentals to Nanoscale Dynamics* (Berlin: Springer)
- [22] Ovchinnikov Y N and Kresin V Z 2003 Relaxation cascade in solids: microscopic theory *Eur. Phys. J. B* **32** 297–302
- [23] Kutnyakhov D *et al* 2013 Imaging spin filter for electrons based on specular reflection from iridium (001) *Ultramicroscopy* **130** 63–69
- [24] Altarelli M, Brinkmann R, Chergui M, Decking W, Dobson B, Düsterer S, Grübel G, Graeff W, Graafsma H, Hajdu J *et al* 2006 The European x-ray free-electron laser *Technical Design Report, DESY* **97** 1–26